ELSEVIER

Polymer 43 (2002) 6585–6593

polymer

www.elsevier.com/locate/polymer

Role of entanglement in nucleation and 'melt relaxation' of polyethylene

Shinichi Yamazaki[a], Masamichi Hikosaka[a,*], Akihiko Toda[a], Isao Wataoka[b], Fangming Gu[b]

[a]*Faculty of Integrated Arts and Sciences, Hiroshima University, 1-7-1 Kagamiyama, Higashi, Hiroshima 739-8521, Japan*
[b]*Venture Business Laboratory, Hiroshima University, 2-313 Kagamiyama, Higashi, Hiroshima 739-8527, Japan*

Received 27 May 2002; received in revised form 18 July 2002; accepted 7 August 2002

Abstract

An experimental formula of the nucleation rate I of polyethylene as a function of number density of entanglement ν_e within the melt was obtained as $I(\nu_e) \propto \exp(-\gamma\nu_e)$, where γ is a constant. In order to obtain a functional form of $I(\nu_e)$, I is determined by changing ν_e within the melt. The ν_e within the melt can be changed when crystals with different lamellar thickness l are melted. It is shown that the ν_e within the melt just after melting is related to l before melting. The ν_e of folded chain crystals (FCCs) is large, while that of extended chain single crystals (ECSCs) is very small. Therefore, strictly speaking, the experimental formula is a kind of 'semi-experimental' one. Because it is obtained by combining an experimental formula of I as a function of l before melting $I(l)$ and a formula between l and ν_e based on the most probable model. It was found that the ν_e dependence of I is mainly controlled by the topological diffusion process within the interface between the melt and a nucleus and/or within the nucleus not by the forming process of a critical nucleus. The slope of the plots of log I against ΔT^{-2} was constant, irrespective of morphologies, FCCs and ECSCs, where ΔT is the degree of supercooling. From this fact, it was concluded that the fold type nucleus are formed from the melt of ECSCs as well as from the melt of FCCs. In our previous study, we found that I decreases exponentially with increase of annealing time Δt at a temperature above the melting temperature. From these results, we proposed a 'two-stage melt relaxation', i.e. fast conformational and slow topological relaxations. When the ECSCs are melted, extended chains within ECSCs are rapidly changed to random coiled chain conformation and then chains gradually entangle each other. We also proposed a formula, $\nu_e(\Delta t) \propto -\ln\{\text{const.} + A\exp(-\Delta t/\tau_m)\}$, where A is a constant and τ_m is the 'melt relaxation' time. © 2002 Published by Elsevier Science Ltd.

Keywords: Nucleation; Melt relaxation; Entanglement

1. Introduction

1.1. Ideal and actual crystallization and melting

The crystallization and melting are the first order phase transitions. Fig. 1 shows a schematic illustration of crystallization and melting processes of polymers. Ideal crystallization and melting of polymers can be regarded as the transitions between fully entangled Gaussian chain melt (the equilibrium melt) and fully extended chain crystals without entanglements (the ideal crystal). Therefore, the crystallization process is considered to be a process where polymer chains are disentangled within interface between a nucleus and the melt and within a small crystal (nucleus or embryo) and are rearranged into large ideal crystals via chain sliding diffusion [1,2]. The melting is reverse process to the crystallization. This means that the topological nature plays an important role in the polymer crystallization and the melting. Therefore, significant changes of number density of entanglement (ν_e) and the chain conformation should occur during the crystallization and melting. In this paper, ν_e is defined to be unity and zero for the equilibrium melt and for the ideal extended chain single crystals (ECSCs), respectively.

Between two ideal states, 'metastable' crystalline and molten states exist as shown in Fig. 1. Small crystals (nucleus or embryo) or folded chain crystals (FCCs) can be regarded as the metastable crystalline state. Small crystals or FCCs should fully disentangle to grow into ideal ECSCs via chain sliding diffusion in lamellae or interface between a nucleus and the melt [1,2]. Partially entangled random coiled melt or locally ordered melt can be regarded as the metastable molten state. Therefore, actual crystallization and melting is the transition between the metastable melt and crystals.

* Corresponding author. Tel.: +81-824-24-6548; fax: +81-824-21-2652.
E-mail address: hikosaka@hiroshima-u.ac.jp (M. Hikosaka).

0032-3861/02/$ - see front matter © 2002 Published by Elsevier Science Ltd.
PII: S0032-3861(02)00592-X

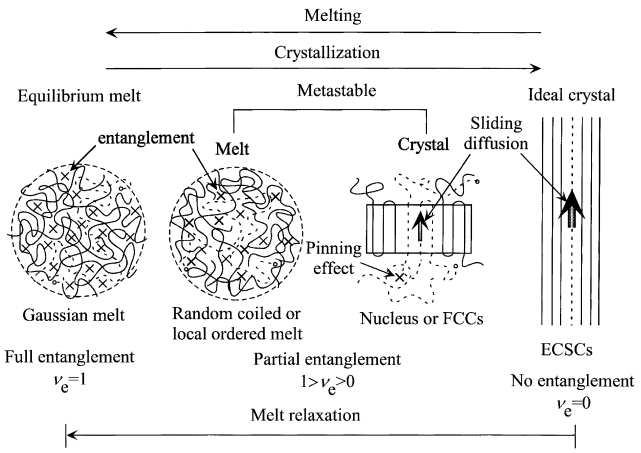

Fig. 1. Schematic illustration of crystallization and melting processes of polymers. Crystallization process corresponds to disentanglement process. Melting process is reverse to crystallization one. Between equilibrium melt and ideal crystal, there exists metastable melt and crystal. Cross-mark denotes the entanglement.

Thus, an important unsolved problem arises; how ν_e and the chain conformation change during the crystallization or melting? Such changes during the melting is sometimes named 'melt relaxation'. We will challenge the unsolved problem in this paper.

1.2. Important role of topological nature in nucleation

One of the authors (MH) has proposed the chain sliding diffusion theory to explain the topological mechanism of crystallization of polymers [1,2]. The theory predicts that the crystallization of polymers is crucially controlled by the topological nature.

Recently, we found a 'power law of the nucleation rate (I)' of single crystals of polyethylene (PE), $I \propto M_n^{-H}$, where M_n is the number averaged molecular weight and H is a constant [3,4].

It was found that H depends on crystalline phase, that is $H = 1.0$ for orthorhombic (ordered) and $H = 2.4$ for hexagonal (disordered) phase, respectively. In the hexagonal phase, polymer chain can easily slide along the chain axis in the crystal due to loose packing. On the other hand, in the orthorhombic phase, polymer chain cannot slide so much due to close packing. Thus, it was concluded that polymer chains should be disentangled within the interface and slide within the crystalline lattice during the nucleation. This clearly showed that the self-diffusion of chain within the melt is not a dominant factor in nucleation and that the chain sliding diffusion and disentanglement play important roles in the nucleation of polymers.

Moreover, we reported that unsolvable entanglements are accumulated on the interface between a crystal and the melt when nucleus grows via chain sliding diffusion [5]. This result suggests again that the entanglement is one of the most important factors in the nucleation.

However, the actual mechanism of disentanglement has not been solved yet. Therefore, determination of I as a function of ν_e is one of the most important unsolved problem. In this paper, we will show $I(\nu_e)$ experimentally.

1.3. Relationship between I and ν_e

When a nucleus is formed and grows via chain sliding diffusion, the entanglements within the interface result in 'pinning effect' as shown in Fig. 1. As a result, the chain sliding diffusion within the nucleus or interface should be suppressed by the entanglements. Therefore, it is expected that I becomes small with increase of ν_e.

According to the chain sliding diffusion theory of nucleation [3], I is expressed by two competing factors

$$I = I_0 \exp(-\Delta G^*/kT) = I_0 \exp(-C/\Delta T^2), \quad (1)$$

where I_0 and C are constants, ΔT is the degree of supercooling, k is the Boltzmann constant and T is the temperature. I_0 is related to topological diffusion constant D as,

$$I_0 \propto D. \quad (2)$$

Whereas, C is proportional to free energy necessary for forming a critical nucleus ΔG^*. In this paper, it will be made clear which factor controls the ν_e dependence of I. It will be shown that the topological diffusion process controls the ν_e dependence of I, while the critical nucleation process does not.

1.4. Effect of melt relaxation on nucleation

We have found recently that I of PE decreases exponentially with increase of annealing time at a temperature above melting temperature (Δt) [6]. Hereafter, we name Δt as 'melt annealing time'. We considered this phenomenon as a kind of melt relaxation. We obtained that I as a function of Δt as

$$I \propto \exp(-\Delta t/\tau_m) + \text{const.} \quad (3)$$

where τ_m is the melt relaxation time.

We have speculated this result that when the melt is kept above the melting temperature, ν_e gradually increases with increase of Δt and approaches equilibrium ν_e ($\nu_e = 1$). It was shown that the melt relaxation process takes long time, i.e. it takes about several hours or a few days depending on annealing temperature (T_{max}) and M_n. However, this experimental fact was an indirect evidence for the role of entanglement in the nucleation of polymers.

1.5. Preliminary evidence of effects of entanglement on nucleation

Psarski et al. [7] have reported the effects of entanglement on the lateral growth of PE. They have shown that the growth rate of the spherulite G of the melt of ECSCs is larger than that of the melt of FCCs. They have considered

that since ν_e of the melt of ECSCs is smaller than that of the melt of FCCs, G of the melt of ECSCs becomes large. However, they did not show the ν_e dependence of G and I. The quantitative ν_e dependences of G and I are important but yet unsolved problems.

Recently, we directly showed a preliminary experimental evidence that I increases with decrease of ν_e [8]. We assumed that ν_e within the melt is changed by changing the lamellar thickness (l) of crystals before melting. This assumption will be proved in detail in Section 2.1. That is, ν_e within the melt decreases with increase of l. We showed that I increases with increase of l for any ΔT. It was suggested that entanglement plays most important role in the nucleation of polymers. However, unsolved problems still remained in our previous study. That is, a formula of I as a function of ν_e, $I = I(\nu_e)$ is unknown.

1.6. 'Melt memory effects' on nucleation

It was found that the melt memory effects are significant in polymers due to the topological nature [9]. It is considered that the melt memory effects are mainly controlled by the following two factors. First, ν_e changes with Δt, i.e.

$$\nu_e = \nu_e(\Delta t), \tag{4}$$

as mentioned in Section 1.4. Second, change of chain conformation during melting. Though it is expected that the chain conformation in the melt significantly affect nucleation, the mechanism has not yet been solved. One of the keys to solve this problem is to observe the nucleation from the melt of ECSCs. Because it is expected that the melt memory effect of this melt is different from that of the melt of FCCs.

1.7. Purpose of this work: relation between I and ν_e and mechanism of two-stage melt relaxation

The first purpose of this work is to propose relation between I and ν_e. From experimental data, we will determine a formula of I as a function of l. Using a relevant model for l dependence of ν_e, we will derive a formula of I as a function of ν_e. Moreover, combining with our previous experimental data, $I(\Delta t)$, we will propose a formula of ν_e as a function of Δt.

The second purpose is to show that the ν_e dependence of I is controlled by the topological diffusion process and not by the critical nucleation process.

The final purpose is to propose a mechanism of 'two-stage melt relaxation' as shown in Fig. 2. We will clarify the change in chain conformation during the melting. We will show that the melt relaxation consisted of a fast conformational and a slow topological changes.

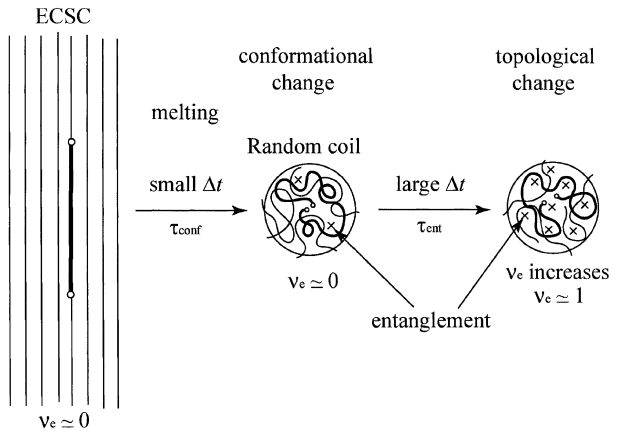

Fig. 2. Schematic illustration of model of two-stage melt relaxation. When ECSCs are melted, the chains within ECSCs are rapidly changed to random coiled conformation. Then, chains are gradually entangled with each other. Cross-mark denotes the entanglement. τ_{conf} and τ_{ent} are the conformational and topological relaxation time, respectively. Δt is the melt annealing time (see text).

2. Methodology: how to determine $I(\nu_e)$ and observe conformational change?

2.1. How to change ν_e in the melt?

As mentioned in our previous paper [8], it is reasonable that thick ECSCs include little entanglement ($\nu_e \sim 0$), while stacked thin lamellae of FCCs have a lot of entanglements (Fig. 3). Therefore, when thick ECSCs and thin FCCs are melted, the melt should have small ν_e and large ν_e, respectively, for small Δt. This suggests that ν_e should decrease with increase of l. Let us consider the relation between ν_e and l, quantitatively.

The spatial size of entanglement is too large to be included within the crystalline lattice. Therefore, it is reasonable to consider that the entanglements, which is expressed by cross-marks in Fig. 3, exist on the surface of crystal or in the amorphous layers between lamellae and they are not included within the crystal. In our previous study for ECSC of PE [5], we have shown that entanglements were accumulated on the end surface of nucleus. From the experimental fact that lamellar thickening growth rate U of ECSC of PE is independent of l [10], we consider that ν_e on the end surface of nucleus is constant and independent of l. For simplicity, we regard the shape of ECSC as a rectangular parallelepiped shown in Fig. 3. Exactly speaking, ECSC has a tapered shape, as shown in our previous paper [11], and the exact calculation for the tapered shape of ECSC is shown in Appendix A. From above experimental facts, it is considered that ν_e is given by the ratio of volume of crystal to surface area of it as below

$$\nu_e \propto \frac{\text{surface area}}{\text{volume}} = \frac{4al + 2a^2}{a^2 l}, \tag{5}$$

where a is the lateral size of ECSC. Here, we assumed that ν_e in the melt does not change so much from that in the

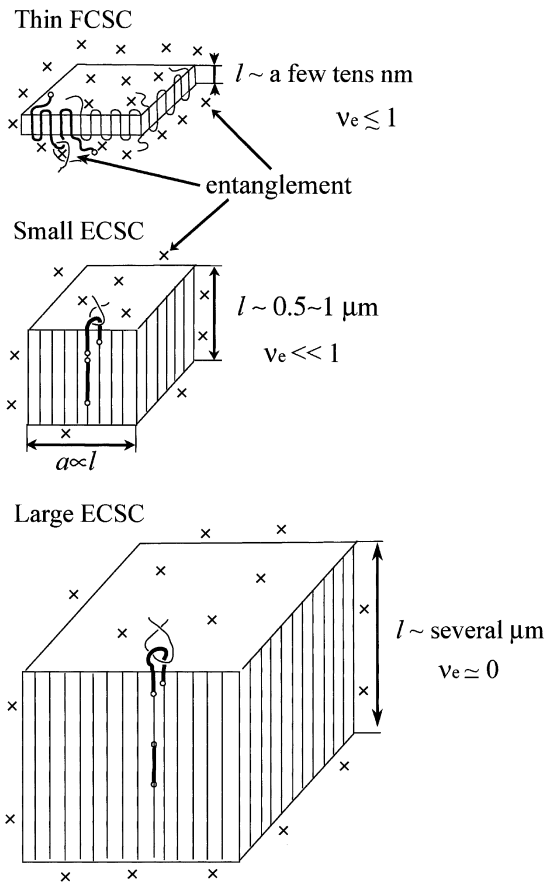

Fig. 3. Schematic illustration of entanglement density for thin FCSC, small ECSC and large ECSC, respectively. Entanglements exist on the surface of crystal or amorphous layers between lamellae. Number density of entanglement ν_e increases with increase of the lamellar thickness l.

crystals if Δt is very small, such as a few minutes as mentioned in Section 1.4.

Since we have shown in our previous study that U is proportional to lateral growth rate V [10], we obtain the following equation,

$$l \propto a. \tag{6}$$

Here, $l \gg l^*$ and $a \gg a^*$ are assumed, where l^* and a^* are critical lamellar thickness and critical lateral size, respectively.

Combination of Eqs. (5) and (6) gives

$$\nu_e(l) = \frac{\beta}{l} \propto \frac{1}{l}, \tag{7}$$

where β is a constant.

2.2. Relation between I and ν_e

A formula of I as a function of ν_e can be obtained by the following steps.

We will obtain the experimental formula of I as a function of l

$$I = I(l). \tag{8}$$

By substituting Eq. (7) in (8), we obtain the formula of $I(\nu_e)$,

$$I = I(\nu_e). \tag{9}$$

2.3. How to prepare ECSCs with different l?

In the case of PE, we can prepare ECSCs with different l using established technique [12] as shown below. Pressure–temperature (P–T) phase diagram consisted of liquid, hexagonal and orthorhombic phases [12–15]. When PE is isothermally crystallized at relevant crystallization temperature (T_c) under the triple point pressure, ECSCs are generated in metastable hexagonal phase [10–12,16–18]. In the hexagonal phase, l of ECSC increases linearly with increase of crystallization time (t) [10,11]. After some time, lamellar thickening growth is stopped when the metastable hexagonal phase transforms into the most stable orthorhombic phase [18]. It was shown that l decreases with decrease of T_c or increase of ΔT. From these mechanisms, we can prepare ECSCs with different l by controlling P, ΔT and t.

2.4. How does chain conformation in the melt change during melting?

How does the chain conformation change from extended chain conformation to random coiled one during melting? We can discuss the chain conformation in the melt from following three criterions.

(1) *Chain conformation can be judged from the type of nucleus generated*. Fig. 4 schematically shows that fold type

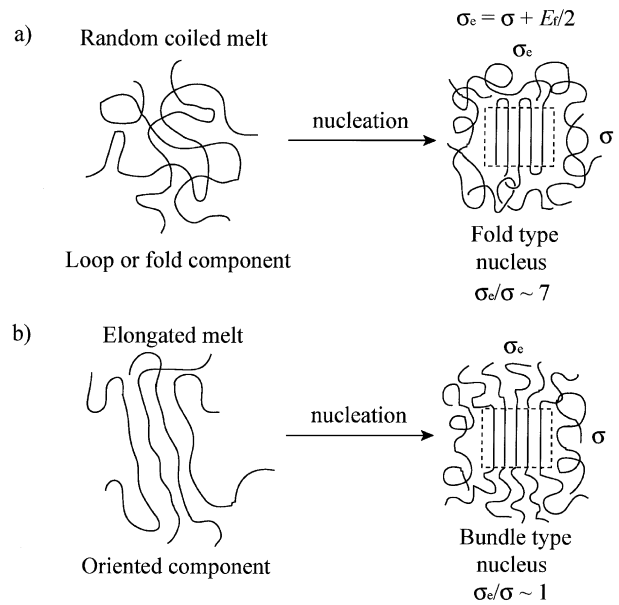

Fig. 4. Schematic illustration of origin of fold and bundle type nucleus. Fold and bundle type nucleus will be formed from random coiled and elongated melt, respectively. The value of end surface free energy σ_e is written by $\sigma_e = \sigma + E_f/2$ [21,22], where σ is side surface free energy and E_f is the energy necessary for forming a sharp folding.

nuclei will be formed from random coiled melt, while bundle type nuclei will be formed from elongated melt. It is noted here that chains in the elongated melt are partially oriented as shown in Fig. 4. We call such melt as the elongated melt. Since chains in the random coiled melt have a lot of fold or loop components, fold or loop have been regarded as the trigger of generation of fold type cluster, embryo or nucleus [19]. Therefore, in the field of polymer crystallization, it is accepted that if fold type nuclei will be formed, the chain within the melt should be randomly coiled.

On the other hand, since some chains are oriented with each other in the elongated melt, it has been considered that bundle type nucleus is generated from the melt [19].

It is an important problem that when ECSCs will be melted, how do chains within ECSCs change from extended chain to random coil? We will make clear which kind of conformation, i.e. random coiled or elongated, can be observed within the melt.

(2) *Type of nucleus can be judged from end surface free energy* (σ_e). The crucial difference between fold and bundle type nuclei is the value of end surface free energy (σ_e) owing to the difference in the structure of end surface. As shown in Fig. 4, it is well known in the case of PE that the ratio of σ_e to side surface free energy σ (σ_e/σ) for fold and bundle type nucleus are 7 and 1, respectively [20]. Therefore, we can experimentally evaluate the type of nucleus from the value of σ_e.

(3) *The value of* σ_e *can be estimated from* $\Delta G^*(\Delta T)$. In Eq. (1), C for heterogeneous nucleation is defined by [5,19]

$$C \equiv \frac{16\sigma\sigma_e\Delta\sigma(T_m^0)^2}{kT\Delta h^2}, \tag{10}$$

where Δh is the enthalpy of fusion, T_m^0 is the equilibrium melting temperature and $\Delta\sigma$ is a constant determined by the kind of nucleating agents or heterogeneity.

It is well known in the case of PE that the value of σ is similar to that for fold type nucleus ($\sigma \sim 14 \times 10^{-3}$ J/m^2) [20] and that for bundle type one. Therefore, difference between fold type and bundle type nucleus can be distinguished by

$$C \propto \sigma_e. \tag{11}$$

From the above three steps, we can clarify the chain conformation in the melt, based on the type of nucleus formed.

3. Experimental

3.1. Sample preparation

Fractionated PE (NIST, SRM1483, $M_w = 3.2 \times 10^4$, $M_w/M_n = 1.11$) was used in this study, where M_w is the weight averaged molecular weight. In order to prepare ECSCs with different l, PE was isothermally crystallized at $\Delta T(h) = 5.5$–13 K under high pressure, $P = 0.4$ GPa using high pressure-differential thermal analysis apparatus [15]. Here, $\Delta T(h)$ is defined by

$$\Delta T(h) \equiv T_m^0(h) - T_c, \tag{12}$$

where $T_m^0(h)$ is the equilibrium melting temperature of hexagonal crystals. FCCs were isothermally crystallized at the atmospheric pressure. The value of l was estimated by transmission electron microscopy.

3.2. Measurements of nucleation rate, I

As schematically shown in Fig. 5, ECSCs or FCCs were melted at 160 °C for 5 min at atmospheric pressure. After that, samples were isothermally crystallized at various T_cs. Hereafter, we abbreviate these processes as ECSCs–melt–FCSC or FCCs–melt–FCSC, respectively, where FCSC means folded chain single crystal. The range of ΔT was about 10–14 K. We used the value of T_m^0 (139.5 °C) reported by Okada et al. [23].

We observed the number density of FCSCs by means of polarizing optical microscope. The number of single crystals should correspond to that of nucleus. Therefore, the number density of nucleus ν was estimated from that of single crystals. I is obtained by

$$I \equiv \frac{d\nu}{dt}. \tag{13}$$

3.3. Instruments

In order to observe nucleation behaviors clearly and evaluate I easily, we have developed a new system combined digital video camera (Victor JVC KY-F70, image size: 1.3M pixels) and hot stage (Linkam LK600PM). Main feature of this combined system is to be controlled by a computer. In this work, Planetron Co. Ltd,

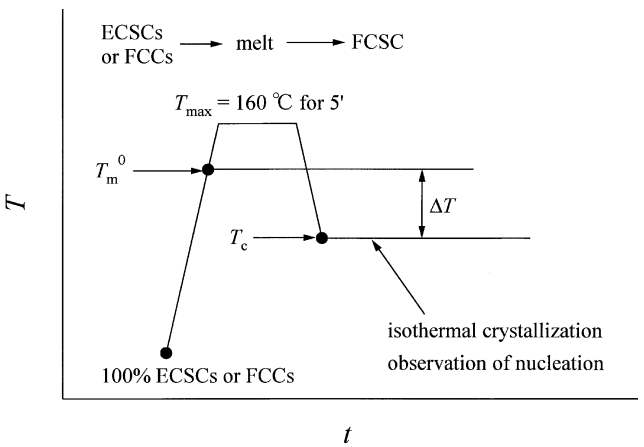

Fig. 5. Schematic illustration of temperature T programming against time t. Hundred percent of ECSCs or FCCs are melted and then kept at T_{max} for 5 min. After that, their melts are cooled to T_c to observe the nucleation.

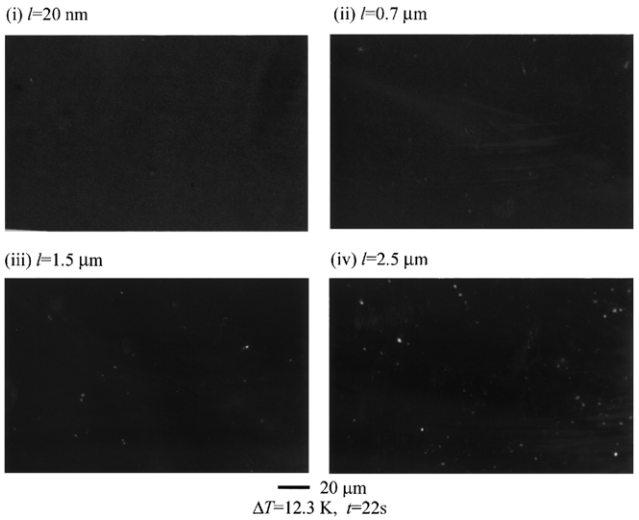

Fig. 6. Typical polarizing optical micrographs of the crystals formed from the melt of samples with different l before melting. At same $t = 22$ s, number density of FCSC is significantly different.

Japan High Tech Co. Ltd and we have a developed new software which is able to control both hot stage and image capturing. Both hot stage and image capturing control software and image analysis software (Media Cybernetics, Image-pro plus) are installed to the computer. The computer is connected to both digital video camera and hot stage controller. The computer receives time and temperature information from the hot stage controller. The received information is automatically superimposed to the image captured from the digital video camera. Using our system, we can obtain sharp images and easily count the number of isolated crystals by Image-pro plus.

4. Results

4.1. Morphology

Typical optical morphology of crystals formed from the melt of samples with different l (ECSCs-melt-FCSC or FCCs-melt-FCSC) for the same t is shown in Fig. 6. Isolated crystals were observed in all samples. It seems that the morphology is the same as reported by Toda [24], irrespective of the morphology before melting. As shown in Fig. 7, it was found that ν increases linearly with increase of t for all the samples, i.e. steady nucleation process.

4.2. Nucleation rate

Fig. 8 shows the plot of log I against ΔT^{-2} for different l. I showed well known Eq. (1) as $I = I_0 \exp(-C/\Delta T^2)$. These straight lines were parallel to each other. This indicates that the slope of the straight line C is almost constant irrespective of l. Moreover, the straight line shifts upward with increase of l. Thus, it is concluded that $I \propto I_0$ increases

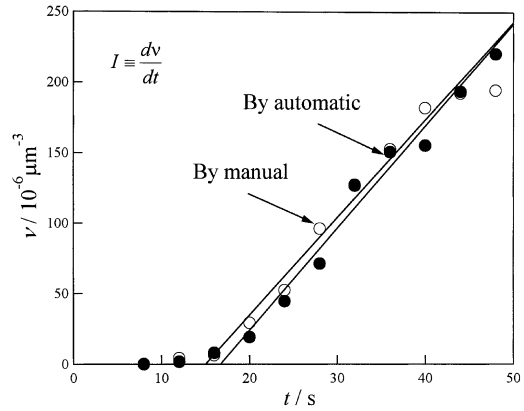

Fig. 7. Comparison between determination of I by manual and automatic methods. Manual and automatic mean counting by conventional method and by computer aided one, respectively. Both methods are almost the same. Number density of nucleus ν increases linearly with increase of t.

with increase of l for any ΔT. Since I_0 and C are proportional to D and ΔG^*, respectively, it is concluded that the l dependence of I is mainly determined by the diffusion process of polymer chain not by the formation process of a critical nucleus.

5. Analysis

5.1. Formulae of $I(l)$, $I(\nu_e)$ and $\nu_e(\Delta t)$

5.1.1. l dependence of I

Fig. 9 shows plot of $I_0(\propto I)$ against l. It was found that $I_0(\propto I)$ increases gradually at first and then rapidly with increase of l. We obtained the following experimental formula of I as a function of l

$$I(l) \propto I_0(l) \propto \exp(-\alpha/l), \tag{14}$$

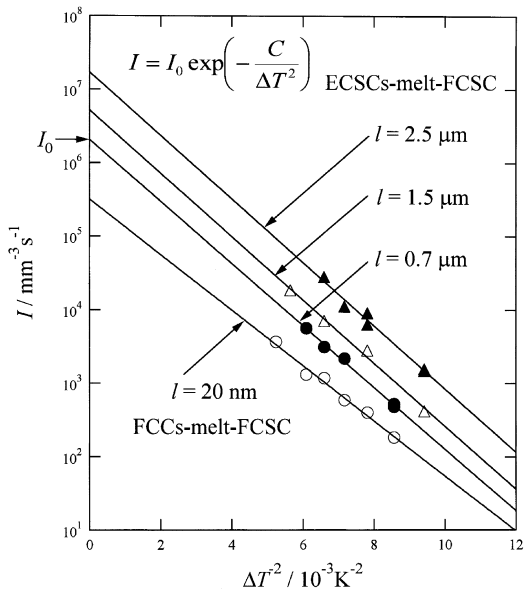

Fig. 8. Plots of log I against ΔT^{-2} for different $l = 20$ nm, 0.7 μm, 1.5 μm, 2.5 μm, respectively. The solid lines show the best fit of the plots.

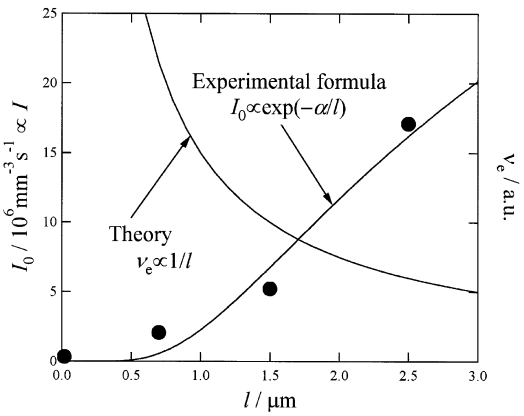

Fig. 9. Plots of $I_0(\propto I)$ against l. The experimental formula is obtained by fitting to experimental data. The other solid curve shows the equation $\nu_e \propto 1/l$.

where α was

$$\alpha = 3.27 \pm 0.17\ \mu\text{m}. \tag{15}$$

5.1.2. ν_e dependence of I

An experimental formula of I as a function of ν_e was obtained for the first time from the combination of Eqs. (7) and (14)

$$I(\nu_e) \propto I_0(\nu_e) \propto \exp\left(-\frac{\alpha}{\beta}\nu_e\right) = \exp(-\gamma\nu_e), \tag{16}$$

where γ is a constant. Fig. 10(a) shows the plots of I_0 against ν_e. The experimental data is fitted with Eq. (16).

The formula of $I(\nu_e)$ indicates that I exponentially decreases with increase of ν_e as shown in Fig. 10(b). It is concluded that nucleation is suppressed by entanglement.

As shown in Fig. 1 and mentioned in Section 1.3, chain sliding diffusion becomes difficult due to pinning effect within the interface between a nucleus and the melt. From Eqs. (2) and (16), the topological diffusion constant is related to ν_e,

$$D(\nu_e) \propto \exp(-\gamma\nu_e). \tag{17}$$

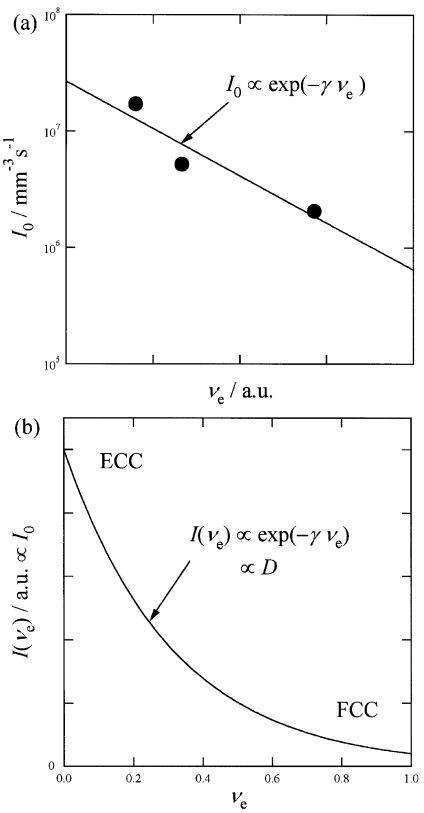

Fig. 10. (a) Plots of I_0 against ν_e. The experimental data is fitted with Eq. (16). (b) The function of $I(\nu_e)(\propto I_0)$ exponentially decreases with increase of ν_e. ECC and FCC in the figure correspond to morphologies before melting, where ECC and FCC mean extended chain crystal and folded chain crystal, respectively.

5.1.3. Δt dependence of ν_e

As mentioned in Section 1.4, we have already obtained the experimental formula between I and Δt as Eq. (3). Combination of Eqs. (3) and (16) gives the formula

$$\nu_e(\Delta t) \propto -\ln\{\text{const.} + A\exp(-\Delta t/\tau_m)\}, \tag{18}$$

where A is a constant.

This equation can be approximated for limit cases,

$$\nu_e \propto \Delta t \qquad \text{for small } \Delta t, \tag{19}$$

$$\nu_e \cong \text{const.} \qquad \text{for large } \Delta t. \tag{20}$$

Fig. 11 shows plot of ν_e against Δt as derived in Eq. (18). This figure also shows the experimental $I(\Delta t)$. We found that decrease of $I(\Delta t)$ with increase of Δt correspond to increase of $\nu_e(\Delta t)$ with increase of Δt. Therefore, it is concluded that increase of ν_e with increase of Δt should be the important mechanism of melt memory effect.

5.2. Two-stage melt relaxation

5.2.1. C does not depend on l

In order to confirm that C is independent of l quantitatively, plot of C against l is shown in Fig. 12. It is

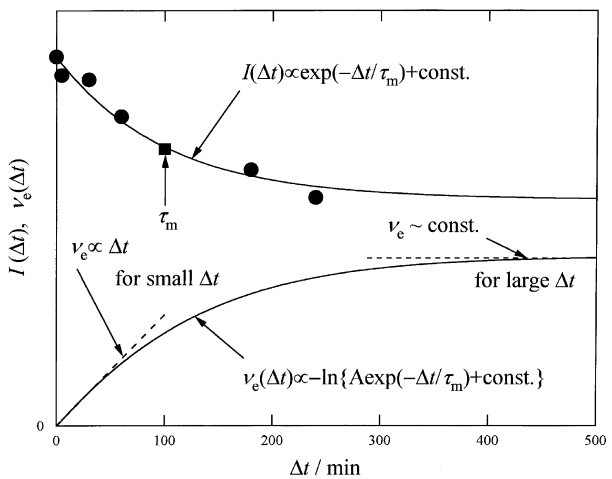

Fig. 11. Plots of I and ν_e against Δt. Decrease of I with increase of Δt corresponds to increase of ν_e with increase of Δt.

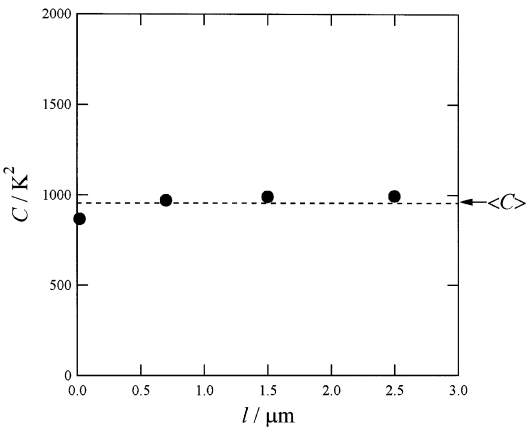

Fig. 12. Plots of C against l. The broken line shows averaged value $\langle C\rangle$.

clearly shown that C does not depend on l. We obtained the average of C ($\langle C\rangle$),

$$\langle C\rangle \cong 955 \pm 30\ (\mathrm{K}^2). \tag{21}$$

Since C is proportional to ΔG^* as mentioned in Section 1.3, ΔG^* is a constant irrespective of l. Therefore, σ_e is also a constant irrespective of l.

5.2.2. Fold nucleus is formed from FCCs-melt and ECSCs-melt

In the case of ordinary melt crystallization such as FCCs-melt-FCSC, a fold type nucleus is formed as mentioned in Section 2.4. Therefore, it is concluded that the fold type nucleus should be also formed from ECSCs-melt because the σ_e is constant irrespective of l, i.e. morphology before melting.

5.2.3. Mechanism of two-stage melt relaxation

In Section 4.4.2, we have shown that the fold type nucleus is formed from the melt of ECSCs. As mentioned in Section 2.4, if the fold type nucleus will be formed from the melt, the chain conformation within the melt should be random coiled one. Therefore, the chain conformation within the melt of ECSCs should be random coiled one. The crucial difference between the melts of ECSCs and FCCs at small Δt is ν_e only. From these considerations, for the melting of ECSCs, we will propose a two-stage melt relaxation consisted from conformational and topological changes as shown in Fig. 2. The chain conformation rapidly changes from the extended one to the random coiled one when ECSCs are melted. Then, chains will gradually entangle each other with increase of Δt and the ν_e will approach the equilibrium one ($\nu_e = 1$). Therefore, the conformational relaxation time (τ_{conf}) is much smaller than the topological relaxation time (τ_{ent}),

$$\tau_{conf} \ll \tau_{ent}. \tag{22}$$

5.3. Effects of entanglement on nucleation of polymers

We have shown that only $I_0(\propto D)$ depends on ν_e, while the $C(\propto \Delta G^*)$ does not on ν_e. This means that the topological nature nucleation is reflected only on the kinetic factor (D) not on the thermodynamic factor (ΔG^*) as shown in our previous paper [3,4]. This is an important conclusion for the effects of entanglement on the nucleation of polymers.

6. Conclusion

1. The nucleation rate (I) increases with increase of the lamellar thickness (l), $I(l) \propto I_0(l) \propto \exp(-\alpha/l)$.
2. Combining the experimental formula and relevant model, we have proposed semi-experimental formula between I and the number density of entanglement (ν_e), $I(\nu_e) \propto I_0(\nu_e) \propto \exp(-\gamma\nu_e)$.
3. We proposed a formula of ν_e as a function of the melt annealing time (Δt), $\nu_e(\Delta t) \propto -\ln\{\text{const.} + A\exp(-\Delta t/\tau_m)$.
4. The free energy necessary for forming a critical nucleus (ΔG^*) does not depend on l. Therefore, the fold type nucleus should be formed from either the melts of ECSCs or that of FCCs.
5. A two-stage melt relaxation, i.e. fast conformational and slow topological relaxations is proposed.

Acknowledgements

This work was partly supported by Grant-in-Aid for Scientific Research on Priority Areas B2 (No. 12127205) and Scientific Research A2 (No. 12305062).

Appendix A. Exact calculation of Eq. (7) for an ECSC with tapered shape

As shown in our previous paper [11], it was reported that the ECSC shows tapered shape. Fig. 13 shows the schematic illustration of real ECSC. From the experimental fact [11], it

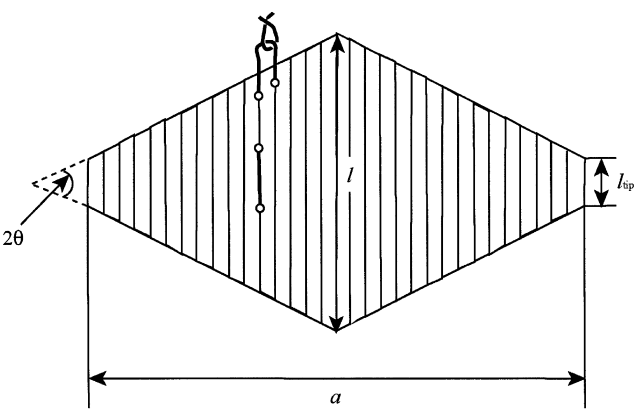

Fig. 13. Schematic illustration of an ECSC with tapered shape.

was shown as

$$l_{tip} \ll l, \tag{A1}$$

$$l_{tip} \ll a, \tag{A2}$$

where l is the maximum lamellar thickness, l_{tip} is the length of tip, a is the lateral size.

The volume of the conical part Φ_1 is given by

$$\Phi_1 = \frac{\pi a^2 (l - l_{tip})}{24}. \tag{A3}$$

The volume of the cylindrical part Φ_2 is given by

$$\Phi_2 = \frac{\pi a^2 l_{tip}}{2}. \tag{A4}$$

Therefore, total volume of a ECSC Φ is given by

$$\Phi = 2\Phi_1 + \Phi_2 = \frac{\pi a^2 l}{12} + \frac{5\pi a^2 l_{tip}}{12}. \tag{A5}$$

Surface area of the cone except for bottom surface S_1 is given by

$$S_1 = \frac{\pi a^2 \cos\theta}{4}, \tag{A6}$$

where θ is the half angle of the taper angle. θ is a constant.

Side surface area of the cylindrical part S_2 is given by

$$S_2 = \pi a l_{tip}. \tag{A7}$$

Therefore, total surface area of a ECSC S is given by

$$S = 2S_1 + S_2 = \frac{\pi a^2 \cos\theta}{2} + \pi a l_{tip}. \tag{A8}$$

Substitution of Eqs. (A1) and (A2) into Eqs. (A5) and (A8) give

$$\Phi \cong \frac{\pi a^2 l}{12} \propto a^2 l, \tag{A9}$$

$$S \cong \frac{\pi a^2 \cos\theta}{2} \propto a^2. \tag{A10}$$

Therefore, the ratio of S/Φ is given by

$$\frac{\text{Surface area}}{\text{volume}} = \frac{S}{\Phi} \propto \frac{1}{l}. \tag{A11}$$

This equation corresponds to Eq. (7).

References

[1] Hikosaka M. Polymer 1987;28:1257–64.
[2] Hikosaka M. Polymer 1990;31:458–68.
[3] Nishi M, Hikosaka M, Ghosh SK, Toda A, Yamada K. Polym J 1999; 31:749–58.
[4] Ghosh SK, Hikosaka M, Toda A. Colloid Polym Sci 2001;279:382–6.
[5] Nishi M, Doctoral thesis, Graduate school of Biosphere Sciences, Hiroshima University 1998.
[6] Gu F, Hikosaka M, Yamazaki S, Toda A. In preparation.
[7] Psarski M, Piorkowska E, Galeski A. Macromolecules 2000;33: 916–32.
[8] Yamazaki S, Hikosaka M, Gu F, Ghosh SK, Arakaki M, Toda A. Polym J 2001;33:906–8.
[9] Alfonso GC, Scardigli P. Macromol Symp 1997;118:323–8.
[10] Hikosaka M, Amano K, Rastogi S, Keller A. J Mater Sci 2000;35: 5157–68.
[11] Hikosaka M, Amano K, Rastogi S, Keller A. Macromolecules 1997; 30:2067–74.
[12] Hikosaka M, Tsukijima K, Rastogi S, Keller A. Polymer 1992;33: 2502–7.
[13] Bassett DC, Block S, Piermarini GJ. J Appl Phys 1974;45:4146.
[14] Yasuniwa M, Enoshita R, Takemura T. Jpn J Appl Phys 1976;15: 1421.
[15] Hikosaka M, Minomura S, Seto T. Jpn J Appl Phys 1980;19:1763–9.
[16] Nishi M, Hikosaka M, Toda A, Takahashi M. Polymer 1998;39: 1591–6.
[17] Rastogi S, Hikosaka M, Kawabata H, Keller A. Macromolecules 1991;24:6384–91.
[18] Hikosaka M, Okada H, Toda A, Rastogi S, Keller A. J Chem Soc, Faraday Trans 1995;91:2573–9.
[19] Price FP. In: Zettlemoyer AC, editor. Nucleation in polymer crystallization. New York: Marcel Dekker; 1969.
[20] Hoffman JD, Frolen LJ, Ross GS, Lauritzen Jr. JI. J Res NBS 1975; 79A:671–99.
[21] Corradini P, Petraccone V, Allegra G. Macromolecules 1971;4: 770–1.
[22] Dave RS, Farmer BL. Polymer 1988;29:1544–54.
[23] Okada M, Nishi M, Takahashi M, Matsuda H, Toda A, Hikosaka M. Polymer 1998;39:4535–9.
[24] Toda A. Colloid Polym Sci 1992;270:667–81.